Ecoepidemic models with prey group defense and feeding saturation

Gimmelli, G.; Kooi, B.W.; Venturino, E.

published in
Ecological Complexity
2015

DOI (link to publisher)
10.1016/j.ecocom.2015.02.004

document version
Publisher's PDF, also known as Version of record

Ecological Complexity 22 (2015) 50–58

Contents lists available at ScienceDirect

Ecological Complexity

journal homepage: www.elsevier.com/locate/ecocom

Original Research Article

Ecoepidemic models with prey group defense and feeding saturation

Giacomo Gimmelli [a], Bob W. Kooi [b], Ezio Venturino [a,*]

[a] Dipartimento di Matematica "Giuseppe Peano", Università di Torino, via Carlo Alberto 10, 10123 Torino, Italy
[b] Department of Theoretical Biology, VU University, de Boelelaan 1085, 1081 HV Amsterdam, The Netherlands

ARTICLE INFO

Article history:
Received 22 October 2014
Received in revised form 8 February 2015
Accepted 15 February 2015
Available online

Keywords:
Herd behavior
Disease transmission
Ecoepidemics
Feeding satiation
Local and global bifurcations

ABSTRACT

In this paper we consider a model for the herd behavior of prey, that are subject to attacks by specialist predators. The latter are affected by a transmissible disease. With respect to other recently introduced models of the same nature, we focus here our attention to the possible feeding satiation phenomenon. The system dynamics is thoroughly investigated, to show the occurrence of several types of bifurcations. In addition to the transcritical and Hopf bifurcation that occur commonly in predator–prey system also a zero-Hopf and a global bifurcation occur. The Hopf and the global bifurcation occur only in the disease-free (so purely demographic) system. The latter is a heteroclinic connection for the between saddle equilibrium points where a stable limit cycle is disrupted and where the system disease-free collapses while in a parameter space region the endemic system exists stably.

1. Introduction

Diseases commonly occur in nature and affect communities. Their role in the shaping the dynamics of populations has been understood since quite some time, with the development of mathematical models for the forecasting of their effects and their possible control. Classical models in this context are the early works on SIRS (Susceptible-Infected-Recovered-Susceptible) models, but during the past century a wealth of other models have been proposed and studied; we mention only the use of the Monod-Haldane function to model the response of individuals to the spread of epidemics, by lowering their contact rates, or models explicitly including viral agents among the systems' populations, see the review (Hethcote, 2000) for a full account of the field.

Only toward the end of the century epidemic models for populations that vary in time have been introduced, (Busenberg and Driessche van den, 1990; Mena-Lorca and Hethcote, 1992), and this opened up the way for the consideration of disease effects on interacting populations. This has now become an independent field of research, starting from the early papers (Hadeler and Freedman, 1989; Beltrami and Carroll, 1994; Venturino, 1994, 1995). More sophisticated models have then been proposed, (Chattopadhyay and Arino, 1999; Haque and Venturino, 2006), building a field now named ecoepidemiology. For a summary of the first steps into it, see the Part I of (Malchow et al., 2008).

The demographic interactions among populations occupying the same territory have been modeled in various ways, ever since the original investigations of Lotka and Volterra, (Malchow et al., 2008). Other models that are now classical are the Holling–Tanner and Leslie-Gower, (Holling, 1965; Tanner, 1976). In more recent years, the concept of prey group defense has been introduced. Originally, (Freedman and Wolkowicz, 1986), this has been proposed by considerations on possible changes in qualitative properties of the response functions. A recent novel contribution however models the fact that it is the individuals at the edge of the herd that generally suffer the heaviest consequences of the predators' attacks. Therefore only the subpopulation of individuals that occupy the outermost positions of the flock should be accounted for interactions with predators. Its size is easily identified as being proportional to the perimeter of the area occupied by the herd. This ultimately depends on the square root of the population density, (Ajraldi et al., 2011). The resulting system of differential equations therefore contains a square root term that renders them markedly different from the classical quadratic predator–prey interactions. As a consequence, the dynamics is deeply affected, as this model exhibits limit cycles, which are known to be impossible to arise in the models constructed with bilinear interaction terms. The idea has been further exploited in (Braza, 2012). In the context of predators' behavior see also related concepts in (Cosner et al., 1999).

* Corresponding author. Tel.: +39 0116702833.
E-mail address: ezio.venturino@unito.it (E. Venturino).

http://dx.doi.org/10.1016/j.ecocom.2015.02.004
1476-945X/

The combination of both the above ideas, namely disease affecting interacting populations and herd behavior, has been explored first in (Venturino, 2011), a study in which the epidemic is assumed to affect the prey, and then in (Belvisi and Venturino, 2013), for the case of diseased predators. In plankton dynamics, this idea has been explored in (Chattopadhyay et al., 2008; Romano et al., 2014), where it is assumed that toxic phytoplankton agglomerates in patches and releases poison through their surface.

Here we want to make a step further, considering also the satiation effect experienced by predators when one type of prey is available in large quantities. After a certain time, the predators disregard the too much abundant food, so that their hunting rate becomes smaller. This phenomenon was firstly modeled in the context of chemical reactions, it is the well-known Michaelis-Menten type dynamics. Later on, in mathematical biology, it has been renamed as Holling type II response function. Here we study this type of situation, combined with the prey gathering together for self-defense purposes. The situation was first proposed in (Gimmelli, 2012) and thoroughly elaborated here, accounting for the epidemics affecting the predators and thereby extending the model (Belvisi and Venturino, 2013). The field evidence of a maximal possible intake of food in a given timespan represents a major reason for proposing this investigation, in that the present model is more adherent to what in fact happens in reality. For drifting herbivores in the savannas, moving in very large herds and subject to individual attacks of predators, the likelyhood that they are hunted in the way we describe here is evident. On the other hand, it is well-known also that a large predator after capturing and ingesting a prey, needs some time to digest it, during which the animal remains inactive, from the hunting point of view. A renowned example is provided for instance by the large snakes, after killing a small mammal they remain idle for quite a bit of time, ranging up to a couple of weeks.

The model is analyzed using bifurcation theory (Guckenheimer and Holmes, 1985; Wiggins, 1988, 1990; Kuznetsov, 2004), where the asymptotic behavior of the system (equilibria, periodic cycles, chaos) is evaluated under parameter variation for qualitative changes. A qualitative change in the asymptotic behavior is then referred to as a bifurcation point. For examples of ecological applications in general we refer to (Bazykin, 1998; Kooi, 2003) and references therein. The organizing center of the bifurcation pattern of the model is a point where transcritical, zero-Hopf and Hopf bifurcations intersect. Also a global bifurcation occurs namely a between two saddle equilibrium points. For analysis techniques of this type of heteroclinic connection see (van Voorn et al., 2010).

The paper is organized as follows. We present at first the pure demographic model, since we will need to compare the final results of the ecoepidemic model against its behavior. It is analyzed in Section 2, as on its own it is a new model, differing, as we discussed above, from the classical Holling type II model because it contains the square root term for group defense. It also differs from the herd behavior model presented in (Ajraldi et al., 2011), because it takes into account the feeding satiation phenomenon. In Section 3 we move then to the case of the predators being affected by the disease. In Section 4, the full bifurcation analysis is carried out, completed for the special instance of codimension two bifurcations in Section 5. A final discussion concludes the paper.

2. The interacting population model

We begin with the pure demographic model presentation and analysis, for later comparison purposes. Per se, this is already a new model, extending the basic models considered in (Ajraldi et al., 2011; Belvisi and Venturino, 2013) to the case of feeding satiation coupled with group behavior. There is therefore also an intrinsic interest in its analysis. In broad lines, the ecosystem under consideration can be described as two populations living in the same environment, each however with different demographic characteristics. In particular the predators behave individually, while the prey instead gather together looking for pastures. Their whole population therefore occupies a contiguous piece of ground. The basic assumption underlying these types of models, (Ajraldi et al., 2011; Belvisi and Venturino, 2013), states that only, or essentially the majority, of the individuals being attacked by the predators will be located at the edge of the territory on which the prey reside. The number of the victims of the attacks will therefore be proportional to the length of a narrow stripe around the boundary of the herd. Since this is essentially a one-dimensional manifold, it is related to the area occupied by the herd via a square root function. The same relationship must therefore hold between the number of individuals suffering attacks at the boundary and the whole prey population. Further, it is widely recognized that an expression of the food intake better than the standard quadratic interactions of the Lotka–Volterra model is represented by the well-known Michaelis–Menten or otherwise called Holling type II response function, in that it sets an upper bound on the possible daily prey consumption. Assuming that the prey reproduce logistically, and that predators are specialists, i.e. they do not have other food sources, and have a bound on the amount of food they can injest per unit time, which is, as mentioned, expressed via the Holling type II response function, we can describe the interactions as follows

$$\begin{aligned}\frac{d}{dt}\widehat{R}(t) &= r\left(1-\frac{\widehat{R}(t)}{\widehat{K}}\right)\widehat{R}(t)-\frac{a\sqrt{\widehat{R}(t)}\widehat{F}(t)}{1+t_h a\sqrt{\widehat{R}(t)}},\\ \frac{d}{dt}\widehat{F}(t) &= -m\widehat{F}(t)+\frac{ac\sqrt{\widehat{R}(t)}\widehat{F}(t)}{1+t_h a\sqrt{\widehat{R}(t)}}.\end{aligned} \tag{1}$$

We remove the singularity that arises in the Jacobian when $\widehat{R}=0$, by setting $\widehat{P}=\sqrt{\widehat{R}}>0$ thus obtaining

$$\begin{aligned}\frac{d}{d\tau}\widehat{P}(\tau) &= \frac{1}{2}\left[r\widehat{P}(\tau)\left(1-\frac{\widehat{P}^2(\tau)}{\widehat{K}}\right)-\frac{a\widehat{F}(\tau)}{1+t_h a\widehat{P}(\tau)}\right],\\ \frac{d}{d\tau}\widehat{F}(\tau) &= -m\widehat{F}(\tau)+\frac{ac\widehat{P}(\tau)\widehat{F}(\tau)}{1+t_h a\widehat{P}(\tau)},\end{aligned} \tag{2}$$

which holds for $\widehat{P}>0$, since in the first equation we have simplified $\widehat{P}$ on both sides. The case $\widehat{P}=0$ corresponds to setting $\widehat{R}=0$ into (1) and therefore obtaining that also the predators vanish exponentially fast. The behavior of this purely demographic model has been discussed in depth in (Braza, 2012), especially for the analysis of the equilibrium with vanishing population. The analysis of (Braza, 2012) however makes the simplifying assumption of a HTI model, i.e. setting $t_h=0$ into (2).

We nondimensionalize it using the following substitutions $P(t)=\alpha\widehat{P}(\tau)$, $F(t)=\beta\widehat{F}(\tau)$, $t=\delta\tau$. We thus find $\frac{d\widehat{P}}{d\tau}=\delta/\alpha dP/dt$, $d\widehat{F}/d\tau=\delta/\beta dF/dt$. Back substitution into (12) gives

$$\begin{aligned}\frac{d}{dt}P(t) &= \frac{1}{2\delta}\left[rP\left(1-\frac{P^2}{\alpha^2\widehat{K}}\right)-\frac{\alpha^2}{\beta}\frac{aF}{\alpha+t_h aP}\right],\\ \frac{d}{dt}F(t) &= \frac{F}{\delta}\left[-m+\frac{acP}{\alpha+t_h aP}\right].\end{aligned} \tag{3}$$

With the choices

$$\beta=\alpha\,,\quad K=\alpha^2\widehat{K}\,,\quad \alpha=t_h a\,,\quad \delta=\frac{1}{2}\,, \tag{4}$$

we obtain the new system

$$\begin{aligned}\frac{d}{dt}P(t) &= rP\left(1-\frac{P^2}{K}\right)-\frac{aF}{1+P},\\ \frac{d}{dt}F(t) &= 2F\left[-m+\frac{1}{t_h}\frac{cP}{1+P}\right].\end{aligned} \tag{5}$$

The equilibria are the points $Q_0=(0,0)$, $Q_1=(\sqrt{K},0)$ and $Q_2=(P_2^d,F_2^d)$ with $F_2^d=ra^{-1}P_2^d(1+P_2^d)(1-(P_2^d)^2K^{-1})$ where, explicitly

$$P_2^d=\frac{mt_h}{c-mt_h},\quad F_2^d=\frac{cmrt_h(c^2K-2cKmt_h-m^2t_h^2+Km^2t_h^2)}{aK(c-mt_h)^4}.$$

For feasibility of the latter, we must impose

$$m\le\min\left\{\frac{c}{t_h},\frac{c}{t_h}\frac{\sqrt{K}}{\sqrt{K}+1}\right\}\equiv\frac{c}{t_h}\frac{\sqrt{K}}{\sqrt{K}+1}\equiv m_d^\dagger. \tag{6}$$

The system (5) has the following Jacobian

$$\begin{pmatrix} r\left(1-\frac{3P^2}{K}\right)+\frac{aF}{(1+P)^2} & -\frac{a}{1+P}\\ \frac{2c}{t_h}\frac{F}{(1+P)^2} & 2\left[-m+\frac{c}{t_h}\frac{P}{1+P}\right]\end{pmatrix} \tag{7}$$

At the origin, the linear stability analysis based on the eigenvalues, $\mu_1=r$, $\mu_2=-2$ m would give instability. However, in (Venturino and Petrovskii, 2013), a narrow stripe around the predators' axis in the phase space is found, for which the trajectories will ultimately approach the origin and the ecosystem would finally disappear. The same conclusion is obtained through a nonlinear stability analysis in the similar simplified HTI model of (Braza, 2012). We will not consider this issue here any longer. At Q_1 we find

$$\mu_1=-2r,\quad \mu_2=2\left[-m+\frac{c\sqrt{K}}{\left(1+\sqrt{K}\right)t_h}\right]$$

so that stability holds if

$$m>m_d^\dagger \tag{8}$$

Proposition 1. Comparing (8) with (6), we see that there is a transcritical bifurcation for which Q_2 emanates from Q_1.

Remark. The predators therefore appear in the ecosystem when the predators' mortality rate falls below the threshold $m_d^\dagger$. Whether they persist in it, depends essentially on the stability conditions of the coexistence equilibrium. Recalling the analysis of (Braza, 2012) mentioned above, the ecosystem could indeed totally disappear.

At Q_2 the Jacobian J_2 is such that

$$det(J_2)=\frac{2c}{t_h}\frac{F_2^d}{(1+P_2^d)^2}\frac{a}{1+P_2^d}>0$$

so that the second Routh–Hurwitz condition holds. For the first one, we have

$$\mathrm{tr}(J_2)=r\left(1-\frac{3(P_2^d)^2}{K}\right)+\frac{aF_2^d}{(1+P_2^d)^2}$$

giving the stability condition

$$\frac{aF_2^d(1+2P_2^d)}{P_2^d(1+P_2^d)^2}<2r\frac{(P_2^d)^2}{K}. \tag{9}$$

When the latter becomes an equality the system possibly exhibits a Hopf bifurcation.

3. The model with disease in the predators

As a reference, consider the model presented in (Belvisi and Venturino, 2013), which we briefly illustrate again here for the convenience of the reader, to better emphasize the changes in our main model. Let $\bar{R}(\tau)$ denote the prey population, let $\bar{F}(\tau)$ be the susceptible predators and $\bar{G}(\tau)$ the diseased predators. Its main feature is the assumptions that prey gather together in herds. When the predators, acting individually, hunt them, it is very likely that the individuals who suffer most from the attacks are those on the outskirts of the herd. They are along the perimeter of the herd, which is distributed over the ground, to occupy a certain surface. The relationship between the occupied surface and its perimeter is then the same that exists between the whole prey population and the subset of its individuals at the edge of the herd. The perimeter, and hence the number of individuals on the border of the herd, is proportional to the square root of the surface, therefore to the whole prey population, since the perimeter is a one-dimensional manifold, while the surface is a two-dimensional one.

Prey reproduce logistically, with growth rate $\bar{r}$ and carrying capacity $\bar{K}$. The healthy predators' hunting rate is $\bar{a}$. The square root term for the prey population accounts for prey gathering in herds. As the number of prey grows, those that are captured are in proportion less, similarly to what happens for Holling-type II response functions.

The predators are partitioned among susceptibles $\bar{F}$, with natural mortality rate $\bar{m}$, and infected $\bar{G}$ whose mortality, natural plus disease-related, is $\bar{n}$. The unrecoverable disease contact rate is $\bar{\lambda}$. The conversion factor of prey into new predators is $0<e\le 1$. The model is

$$\begin{aligned}\frac{d\bar{R}}{d\tau} &= \bar{r}\left(1-\frac{\bar{R}}{\bar{K}}\right)\bar{R}-\bar{a}\sqrt{\bar{R}}\quad \bar{F},\\ \frac{d\bar{F}}{d\tau} &= \bar{F}(-\bar{m}+e\bar{a}\sqrt{\bar{R}}-\bar{\lambda}\ \bar{G}),\\ \frac{d\bar{G}}{d\tau} &= \bar{G}(-\bar{n}+\bar{\lambda}\quad \bar{F}).\end{aligned} \tag{10}$$

We now turn to the model with feeding satiation. Let $\widehat{R}$ denote the prey, $\widehat{F}$ the healthy predators and $\widehat{G}$ the infected predators.

The first equation contains the prey dynamics. The first terms in it state that prey reproduce logistically. The third term models instead hunting by the predators, when the prey gather in herds for defensive purposes.

We assume that only healthy predators reproduce, the diseased ones are too weak for that. The susceptible ones can become diseased by contact with an infectious carrier. By successful contacts healthy predators move into the class of infected ones. The disease is unrecoverable, so that individuals in the infected class can exit it only by dying. Only the healthy predators are strong enough to hunt prey, but exhibit a satiation effect when the food is abundant, modeled by the HTII term, see the last term in the first equation of (11).

A horizontally transmissible disease affects them, so that by successful contacts healthy predators move into the class of infected ones. The disease is unrecoverable, so that individuals in this last class can exit it only by dying.

These facts are mathematically expressed by the following system

$$\begin{aligned}\frac{d\widehat{R}}{d\tau} &= \widehat{r}\widehat{R}\left(1-\frac{\widehat{R}}{\widehat{K}}\right)-\frac{\widehat{a}\sqrt{\widehat{R}}\widehat{F}}{1+\widehat{T}\widehat{a}\sqrt{\widehat{R}}},\\ \frac{d\widehat{F}}{d\tau} &= \widehat{F}\left[-\widehat{m}+\frac{\widehat{e}\widehat{a}\sqrt{\widehat{R}}}{1+\widehat{T}\widehat{a}\sqrt{\widehat{R}}}-\widehat{\lambda}\widehat{G}\right],\\ \frac{d\widehat{G}}{d\tau} &= \widehat{G}\left[-\widehat{n}+\widehat{\lambda}\widehat{F}\right].\end{aligned} \tag{11}$$

The model contains the following parameters: $\widehat{r}$ represents the prey net reproduction rate; $\widehat{K}$ is the prey carrying capacity; $\widehat{\lambda}$ is the disease contact rate; $\widehat{a}$ represents the predators' hunting rate; $\widehat{m}$ is the predators' natural mortality rate; $\widehat{n}$ is the infected predators' mortality rate, i.e. the natural plus disease-related mortality; $\widehat{T}$ denotes the average time to capture a prey; $\widehat{e}$ is biomass conversion factor.

We remove the singularity that arises in the Jacobian when $\widehat{R}=0$, by setting $\widehat{P}=\sqrt{\widehat{R}}\geq 0$ thus obtaining

$$\begin{aligned}\frac{d\widehat{P}}{d\tau} &= \frac{\widehat{r}}{2}\widehat{P}\left(1-\frac{\widehat{P^2}}{\widehat{K}}\right)-\frac{1}{2}\frac{\widehat{a}\widehat{F}}{1+\widehat{T}\widehat{a}\widehat{P}},\\ \frac{d\widehat{F}}{d\tau} &= \widehat{F}\left[-\widehat{m}+\frac{\widehat{e}\widehat{a}\widehat{P}}{1+\widehat{T}\widehat{a}\widehat{P}}-\widehat{\lambda}\widehat{G}\right],\\ \frac{d\widehat{G}}{d\tau} &= \widehat{G}\left[-\widehat{n}+\widehat{\lambda}\widehat{F}\right].\end{aligned} \tag{12}$$

Next, the model is nondimensionalized using the following substitutions $P(t)=\alpha\widehat{P}(\tau)$, $F(t)=\beta\widehat{F}(\tau)$, $G(t)=\gamma\widehat{G}(\tau)$, $t=\delta\tau$.

$$\begin{aligned}\frac{dP}{dt} &= \frac{1}{2\delta}\left[\widehat{r}P\left(1-\frac{P^2}{\alpha^2\widehat{K}}\right)-\frac{\alpha^2}{\beta}\frac{\widehat{a}}{\alpha+\widehat{T}\widehat{a}P}F\right],\\ \frac{dF}{dt} &= \frac{F}{\delta}\left[-\widehat{m}+\frac{\widehat{e}\widehat{a}}{\alpha+\widehat{T}\widehat{a}P}P-\frac{\widehat{\lambda}}{\gamma}G\right],\\ \frac{dG}{dt} &= \frac{G}{\delta}\left[-\widehat{n}+\frac{\widehat{\lambda}}{\beta}F\right].\end{aligned} \tag{13}$$

With the choices

$$\alpha=\widehat{T}\widehat{a},\quad \delta=\frac{1}{2}\widehat{r},\quad \beta=\frac{\widehat{\lambda}}{\widehat{r}},\quad \gamma=\widehat{\lambda},$$

and letting

$$\widehat{r}=2r,\quad \widehat{\lambda}=\lambda,\quad \widehat{e}=e,\quad \widehat{a}=a,\quad \widehat{n}=2rn,\quad \widehat{m}=m,\quad \widehat{K}=K,\quad \widehat{T}=T,$$

we obtain the final system

$$\begin{aligned}\frac{dP}{dt} &= P\left(1-\frac{P^2}{a^2KT^2}\right)-\frac{1}{\lambda}\frac{a^2T}{1+P}F,\\ \frac{dF}{dt} &= \frac{F}{r}\left[\frac{1}{T}\frac{e}{1+P}P-m-G\right],\\ \frac{dG}{dt} &= 2G[F-n].\end{aligned} \tag{14}$$

3.1. Equilibria

The critical points $E_k=(P_k, F_k, G_k)$ that are possibly feasible are now investigated. We find the origin, the zero-solution equilibrium $E_0=(0, 0, 0)$, the prey population equilibrium $E_1=(aT\sqrt{K},0,0)$, the disease-free predator–prey equilibrium $E_2=(P_2, F_2, 0)$, where

$$P_2=\frac{mT}{e-mT},$$

$$F_2=\frac{\lambda P_2(1+P_2)\left(a^2KT^2-P_2^2\right)}{a^4KT^3}=e\lambda m\frac{a^2K(e-mT)^2-m^2}{a^4K(e-mT)^4}$$

with feasibility condition

$$e>mT,\quad m\leq\frac{ae\sqrt{K}}{1+aT\sqrt{K}}\equiv m^{\dagger}. \tag{15}$$

The coexistence equilibrium $E_3=(P_3, F_3, G_3)$ with

$$F_3=n,\quad G_3=\frac{e}{T}\frac{P_3}{1+P_3}-m,$$

and where P_3 is a root of the equation

$$\Psi(P_3)\equiv\frac{\lambda}{a^2KT^2}P_3^4+\frac{\lambda}{a^2KT^2}P_3^3-\lambda P_3^2-\lambda P_3+na^2T=0.$$

By Descartes' rule of signs, there are two real positive roots or none. A sufficient condition for the existence of two positive roots is for instace $\Psi(1)\leq 0$, since $\Psi(0)=na^2T>0$. Explicitly,

$$\frac{1}{a^2KT^2}+\frac{a^2nT}{2\lambda}\leq 1. \tag{16}$$

Evidently for (16) being an equality, the two roots coalesce into $P_3=1$. Feasibility of E_3 is ensured if

$$P_3\geq\frac{mT}{e-mT}. \tag{17}$$

3.2. Stability

The system's Jacobian is

$$\begin{pmatrix}\left(1-\frac{3P^2}{a^2KT^2}\right)+\frac{1}{\lambda}\frac{a^2T}{(1+P)^2}F & -\frac{1}{\lambda}\frac{a^2T}{1+P} & 0\\ \frac{e}{rT}\frac{F}{(1+P)^2} & \frac{1}{r}\left(\frac{1}{T}\frac{e}{1+P}P-m-G\right) & -\frac{F}{r}\\ 0 & 2G & 2(F-n)\end{pmatrix} \tag{18}$$

The eigenvalues at the origin are $\omega_{01}=1$, $\omega_{02}=-m/r$, $\omega_{03}=-2n$, showing its instability.

At E_1 we find instead $\omega_{11}=-2$, $\omega_{12}=r^{-1}(m^{\dagger}-m)$, $\omega_{13}=-2n$. The prey population quilibrium E_1 is thus stable for

$$m>m^{\dagger}. \tag{19}$$

Proposition 2. Comparing (19) and the second (15) we observe a transcritical bifurcation, for which the disease-free predator–prey equilibrium E_2 emanates from the prey population equilibrium E_1 when the latter becomes unstable.

Remark. This happens for the predators' natural mortality crossing from above the critical value $m^{\dagger}$.

The simulations show that indeed the prey population equilibrium E_1 can be stably achieved for instance with the parameter values $a = 0.5, K = 10{,}000, T = 0.45, \lambda = 0.7, n = 0.8, r = 0.7, e = 0.2, m = 0.7$, see Fig. 1.

For E_2 one eigenvalue is $2(F_2 - n)$ and the remaining ones are the roots of a quadratic characteristic equation arising from a 2×2 minor of the Jacobian evaluated at E_2. Note that from the equilibrium equations, the entry $J_{22}(E_2)$ of the Jacobian vanishes. For stability, in addition to

$$F_2 < n, \tag{20}$$

applying the Routh–Hurwitz conditions, we thus need

$$1 + \frac{1}{\lambda}\frac{a^2 T}{(1+P_2)^2}F_2 < \frac{3P_2^2}{a^2 K T^2}, \tag{21}$$

$$\frac{e}{r\lambda}\frac{a^2 F_2}{(1+P_2)^3} > 0. \tag{22}$$

Clearly (22) is always satisfied. Thus stability is achieved when (20) and (21) both hold. In Fig. 2 the equilibrium is achieved, for the parameters $a = 0.2294$, $K = 13.6293$, $T = 2.036$, $\lambda = 1.9807$, $n = 0.1531$, $r = 0.1897$, $e = 0.475$, $m = 0.1476$.

4. Bifurcation analysis

Numerical simulation results are obtained by solving the set of ODE's with ode-solvers available in Matlab (Package, 2014) and a numerical method based on bifurcation theory, see (Kuznetsov, 2004). The numerical bifurcation analysis results are obtained using, AUTO (Doedel and Oldeman, 2009) and MATCONT (Dhooge et al., 2003).

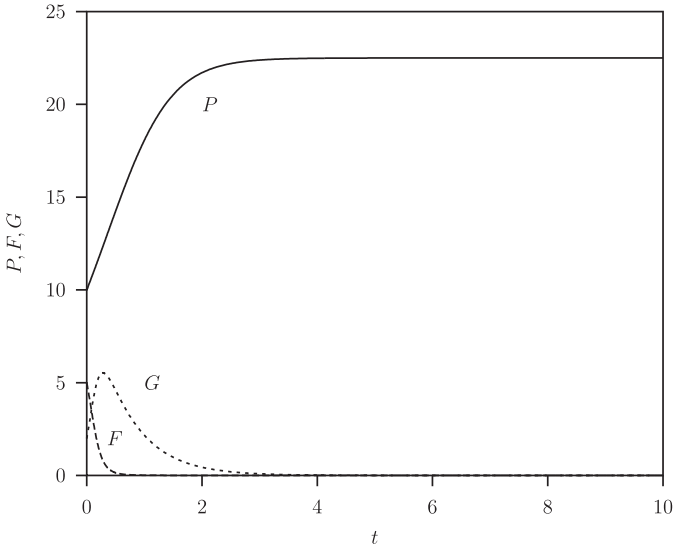

Fig. 1. Solution of endemic system (14) for the three state variables $P \geq 0$ (solid curve), F susceptible predator population (long dashed curve) and G (short dashed curve) the infected predator population, as function of time t. There is convergence to the stable prey population equilibrium E_1 where only the prey population, P, survives. Parameter values used: $a = 0.5$, $K = 10000$, $T = 0.45$, $\lambda = 0.7$, $n = 0.8$, $r = 0.7$, $e = 0.2$, $m = 0.7$.

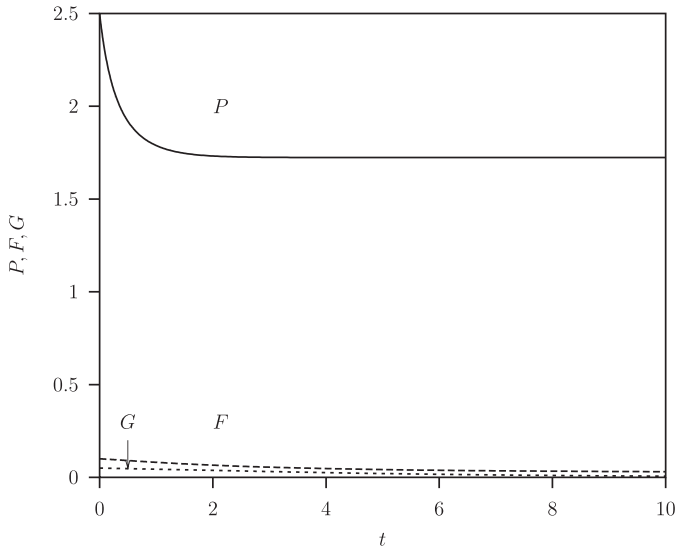

Fig. 2. Solution of endemic system (14) for the three state variables $P \geq 0$ (solid curve), F susceptible predator population (long dashed curve) and G (short dashed curve) the infected predator population, as function of time t. There is convergence to the stable disease-free predator–prey equilibrium E_2 where the prey population, P and the susceptible predator population, F, survive. Parameter values used: $a = 0.2294$, $K = 13.6293$, $T = 2.036$, $\lambda = 1.9807$, $n = 0.1531$, $r = 0.1897$, $e = 0.475$, $m = 0.1476$.

We calculate and continue by varying one parameter, the natural mortality rate of the predators (m) or the carrying capacity (K), equilibria and limit cycles and their stability as well as the location of bifurcation points (critical parameter values), or curves of bifurcation points, when two parameters are varied simultaneously. A list of the symbols for the variables and parameters and the reference parameter values are given in Table 1. Unless otherwise specified, we have used this set of parameter values. When we want to investigate the effect of the disease of the predator population on the system dynamics we vary the unrecoverable disease contact rate λ (results not shown).

Bifurcation analysis results are presented for the model (14) of the predator–prey system with a disease in the predator population formulated and discussed in Section 3. A list of all attractors and bifurcation points and curves is given in Table 2.

The one-parameter bifurcation diagram is shown in Fig. 3 where m is the bifurcation parameter and the parameters are given in Table 1 where $K = 50$. With large mortality rates only the prey population persists. Decreasing the parameter m the susceptible predator population invades at the transcritical bifurcation TC_1 leading to the disease-free predator–prey system PF. For slightly

Table 1
List of symbols for variables and parameters and parameter values used in the text. With this parameter set we have the inequality $m < n$. Consequently, this condition holds for all numerical results presented in this paper.

Symbol	Value	Description
P, F, G	variable	Populations: prey, susceptible predator and infected predator
a	0.5	Hunting rate
e	0.5	Conversion factor of prey into new predators
K	variable	Carrying capacity
m	variable	Natural mortality rate of susceptible-predators, $m < n$
n	0.75	Natural+disease-related mortality of infected-predators
r	0.7	Intrinsic growth rate of susceptible prey
T	0.8	Denotes the average time to capture a prey
t	variable	Time
λ	0.7	Contact rate for the unrecoverable disease

Table 2
List of the equilibrium points and the bifurcations points and curves.

Attractor	Description
E_0	Zero-solution equilibrium
E_1	Prey only equilibrium
E_2	Disease-free predator–prey equilibrium
L_2	Disease-free predator–prey limit cycle
E_3	Endemic predator–prey equilibrium
Bifurcation	**Description**
TC_1	Transcritical bifurcation predator invasion into prey equilibrium
TC_2	Transcritical bifurcation infected predator invasion into susceptible predator equilibrium
ZH	zero-Hopf bifurcation for endemic predator–prey system attractor and repeller equilibrium branches collide
T	Tangent or saddle-node bifurcation collision of two equilibria or limit cycles
H	Hopf bifurcation for disease-free predator–prey system origin of (un)stable limit cycle
$G^{\neq}$	Global bifurcation for disease-free predator–prey system Heteroclinic connection where destruction of limit cycle occurs

lower value the predator population becomes infected, leading to the endemic predator–prey system *PFG*. Decreasing the mortality m further the infected predator population increases while the susceptible predator population and the prey population remain the same. Hence, the disease in the predator population persists endemically for mortality rates below the transcritical bifurcation TC_2.

We now discuss the dynamics of the disease-free predator–prey system *PF*, $G = 0$ (so the purely demographic system). Below the transcritical bifurcation TC_1 this system is unstable. At the Hopf bifurcation, H, an unstable limit cycle L_2 occurs. Lowering m the amplitude of these limit cycles grows fast and it is broken by a heteroclinic connection between two saddle equilibrium points where $F = 0$ at the global bifurcation point $G^{\neq}$, (see also (van Voorn et al., 2007)). However, when there is a outbreak of the disease the system will converge to the stable equilibrium E_3. Then this phenomenon is not relevant. Below we will discover such situations when the carrying capacity K is small and where this phenomenon is relevant.

In Fig. 4 the two-parameter diagram is shown for the endemic predator–prey system *PFG*, where both m and K are varied. It gives the continuation of the two transcritical bifurcations TC_1 and TC_2. Above the curve TC_1 the prey equilibrium E_1 is stable. Between the two curves TC_1 and TC_2 the disease-free predator–prey equilibriun E_2 is stable. The bifurcation TC_2 intersects with the Hopf bifurcation H of the disease-free predator–prey system *PF*. At this intersection point M, denoted by a bullet, a zero-Hopf (or fold-Hopf) bifurcation ZH (vertical) curve for the endemic predator–prey system *PFG* emerges. At that point on the curve for a fixed m while increasing K two coexisting equilibria emerge as is always the case for a tangent bifurcation. Here the bifurcation is a zero-Hopf bifurcation ZH and therefore one branch of equilibria is stable, and an attractor (one negative real eigenvalue and two conjugated complex ones, with negative real parts), and the other branch is unstable, and a repeller (one positive real eigenvalue and two conjugated complex ones with positive real parts). Consequently the unstable branch does not act as a separatrix as is generally the case with tangent bifurcations. Hence in the region below the top branch of the TC_2 curve, the coexistence equilibrium E_3 of the endemic predator–prey system *PFG* is stable. See the results shown in Fig. 3 where $K = 50$. We note that for large K-values equilibrium E_3 is still stable but the real part of the two conjugated eigenvalues of the Jacobian matrix become very close to zero. For instance, for the reference values in Table 1 the real part is -6.24×10^{-7}. This means that the transient dynamics converges very slowly to the stable equilibrium E_3.

What happens close to the origin $K = 0$ and $m = 0$ is studied in the next section where we discuss the unfolding near the degenerated bifurcation *TC-ZH-H* point M where three bifurcation curves collide.

The diagram shown in Fig. 5 where also the stable long-term dynamics is given for the different regimes separated by the co-dim one bifurcation curves, is the blow up of the diagram presented in Fig. 4 now for the low K and low m range.

Observe that in Fig. 5 the transcritical bifurcation TC_2 continues for decreasing m on the same side to the (zero-Hopf) bifurcation ZH line (is nontransversal) and that the Hopf bifurcation point continues crossing this (zero-Hopf) bifurcation ZH line

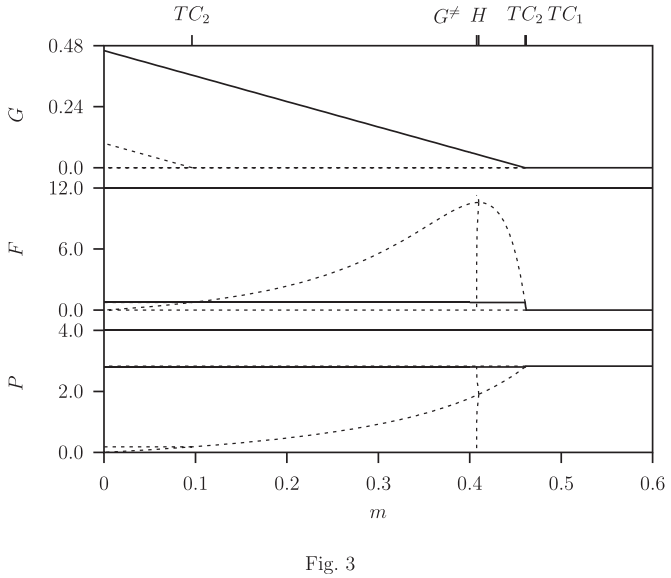

Fig. 3

Fig. 3. One-parameter bifurcation diagram for the endemic system (14) for prey population, P, susceptible predator population, F, infected predator population, G with free parameter m where $K = 50$. All other parameter values are given in Table 1. The solid (dashed) curves denote stable (unstable) equilibrium values. Table 2 gives a list of the bifurcation points.

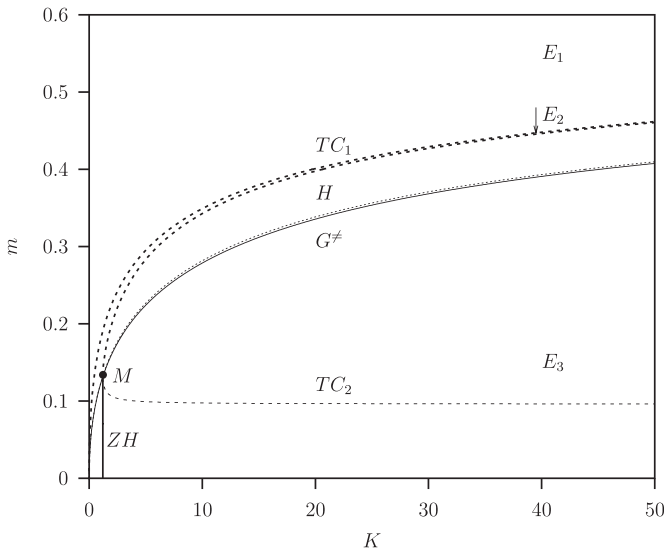

Fig. 4. Two-parameter diagram for parameters carrying capacity, K, and natural mortality, m, of endemic system (14). All fixed parameter values are given in Table 1. Table 2 gives a list of all bifurcation points and curves. The bullet marks a degenerated bifurcation *TC-ZH-H* point M.

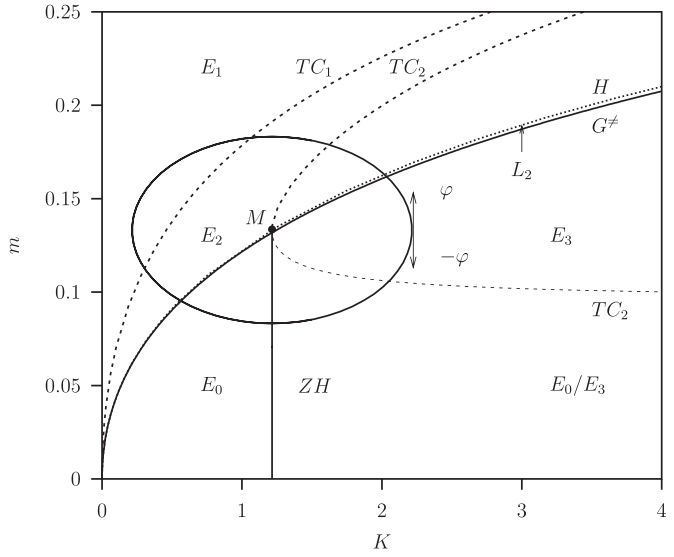

Fig. 5. Two-parameter bifurcation diagram of endemic system (14) with the natural mortality rate of the predators, m, on the vertical-axis, and the carrying capacity, K, on the horizontal-axis. This is a blow up of the diagram presented in Fig. 4 for the region in the neighbourhood of *TC-ZH-H* point M at location ($K^* = 1.2147066$, $m^* = 0.13321752$). The ellipse is defined in (5).

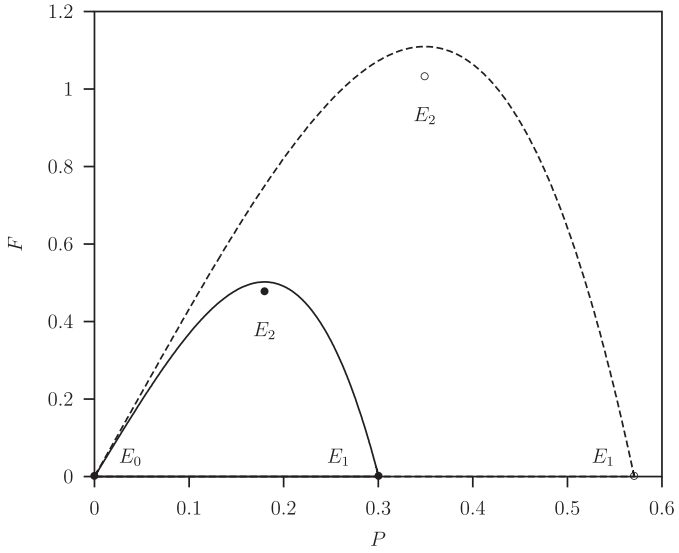

Fig. 6. Heteroclinic connection at two points (solid curve and bullets, and dashed curve and circles) on the ellipse intersection points with the Hopf bifurcation in Fig. 5. This is for the predator–prey disease-free system (14) where $G = 0$. The zero-solution E_0 is connected with a disease-free equilibrium point E_1. In the *PF*-plane the heteroclinic connection curves round the endemic predator–prey system equilibrium E_2.

(is transversal) at its terminal point M. Crossing this M point for the endemic case and following the tangent bifurcation of the endemic *PFG* system, G is zero at M and changes sign, being positive for lower m values.

Starting at this point with $G = 0$ for the disease-free (so the purely demographic) system *PF* where G remains zero, a limit cycle L_2 originates from the Hopf bifurcation H. The amplitude of this limit cycle increases very fast when m is diminished and this stable limit cycle is broken at a global bifurcation at point $G^{\neq}$. The heteroclinic connections for the two global bifurcation points where the ellipse intersects the $G^{\neq}$ curve in Fig. 5 are shown in Fig. 6. We recall that for $K = 50$ discussed above with the description of the results presented in Fig. 3, this phenonemon was not relevant but here it is since for K values below the point M there is no stable endemic equilibrium E_3.

In (van Voorn et al., 2007) a number of numerical techniques are described to calculate these heteroclinic connections and to continue them. Here we used the simplest method: the limit cycle is continued in the two parameter diagram with a large period. Thereafter similar results as those shown in Fig. 6 were obtained and gave convincing results that the calculated global bifurcation curves shown in Figs. 4 and 5 are correct.

In Fig. 7 the population solutions for the parameter combinations, $K = 1$ and $m = 0.05$ are shown. This is in the region in Fig. 5 between the global bifurcation curve $G^{\neq}$ and the vertical zero-Hopf bifurcation indicated by E_0. These results suggest that the prey population P goes first extinct in finite time. The time of extinction depends on the initial conditions. Thereafter the predator populations F, G go extinct asymptotically. We conjecture that this is a result of the possibly non-uniqueness of the solution due to the square root singularity of the ODE that describes the dynamics of the prey population P.

In the region in the parameter space on the right-hand side of the curve *ZH* and below the transcritical bifurcation curve TC_2 we have bistability of E_0 with the endemic predator–prey equilibrium E_3.

5. Transcritical-zero-Hopf–Hopf bifurcation

The position of the transcritical–zero-Hopf–Hopf bifurcation *TC-ZH-H* point M (see Figs. 4 and 5) was found numerically. This

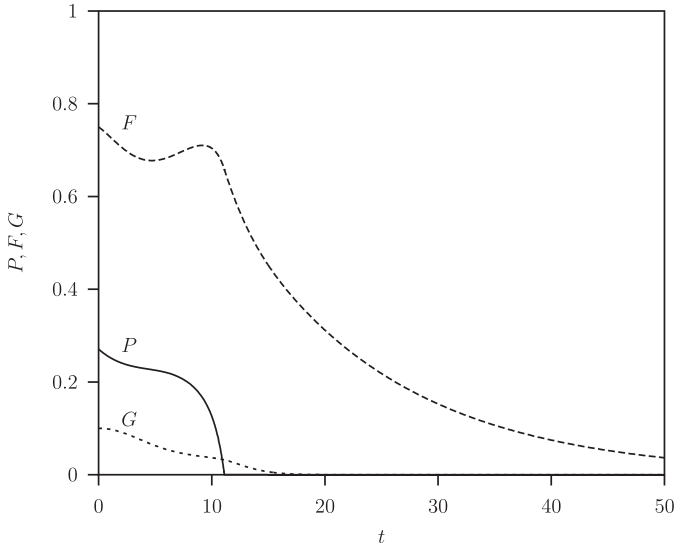

Fig. 7. Solution of the endemic system (14) for the three state variables $P \geq 0$ (solid curve), F susceptible predator population (long dashed curve) and G (short dashed curve) the infected predator population, as function of time t, where $K = 1$ and $m = 0.05$. All fixed parameter values are given in Table 1.

degenerated bifurcation point acts as the organising center being the intersection of three bifurcation curves calculated separately by continuation.

Using MATLAB (Package, 2014) we checked that at this point there is one zero-eigenvalue and two conjugated complex eigenvalues with zero real parts while furthermore the infected predator population gets extinct, $G = 0$, thereby giving a disease-free system *PF*.

In (Saputra et al., 2010) the unfolding of two different types (one or two zero eigenvalues) of tangent–transcritical *T-TC* bifurcations are discussed. In (van Voorn and Kooi, 2013) a one zero eigenvalue example was analyzed. Here the situation is much more complex and we restrict the analysis to a numerical one. In

order to study the unfolding we give in Fig. 8 a one-parameter diagram for the angle $\varphi \in [-\pi, \pi]$ reckoned clockwise in the interval $(-\pi < \varphi < 0)$ and reckoned counter-clockwise in the interval $0 < \varphi < \pi)$ along an ellipse around the *TC-ZH-H* point *M*. This ellipse is shown in Fig. 5 together with the directions of φ and it is described by

$$K = K^* + 1\cos(\varphi)\,, \tag{23a}$$

$$m = m^* + 0.05\sin(\varphi)\,. \tag{23b}$$

where (K^*, m^*) denotes the location of the degenerated bifurcation point *M*.

Starting at $\varphi = 0$ the disease is endemic where the three state variables *P*, *F*, *G* are positive at equilibrium E_3. Continuation in the positive $\varphi > 0$ direction, the system becomes disease-free at the transcritical bifurcation TC_2 at $\varphi = 1.15$ due to epidemiological effects. Starting from this point TC_2 in the negative φ direction the disease-free system is unstable. On this unstable branch a Hopf bifurcation *H* exists at $\varphi = 0.6412$. In this Hopf bifurcation a stable limit cycle originates. The amplitude of this limit cycle increases very fast when *m* is diminished and this limit cycle is broken at the global bifurcation point $G^{\neq}$ $\varphi = 0.6083$ as described above. Continuing with φ in the positive φ direction from TC_2, the predator population goes extinct at the transcritical bifurcation TC_1 at $\varphi = 1.72$ due to pure ecological effects. Starting from this point TC_1 in negative φ direction the prey only system with equilibrium E_1 is unstable and becomes stable again at TC_1 at $\varphi = -2.72$. Continuation from the TC_1 point in the positive φ direction the susceptible predator *F* invades the prey *P* system leading to the disease free system *PF*. This disease free system becomes unstable at the Hopf bifurcation *H* at $\varphi = -2.288$ and, similar to what happened above, the amplitude of the originating stable limit cycle increases fast leading to the collapse at the global bifurcation $G^{\neq}$ at $\varphi = -2.279$.

Continuation from $\varphi = 0$ in the negative direction $\varphi < 0$ firstly at the transcritical bifurcation TC_2 there is bistability of E_3 with E_0. Then, at the catastrophic zero-Hopf bifurcation *ZH* the system collapses completely to E_0. Between point *ZH* and the global bifurcation $G^{\neq}$ in Fig. 8 no stable asymptotic solutions are found and starting in the positive octant of the three dimensional state space *P*, *F*, *G* always leads to a total collapse where the prey population goes extinct in finite time first.

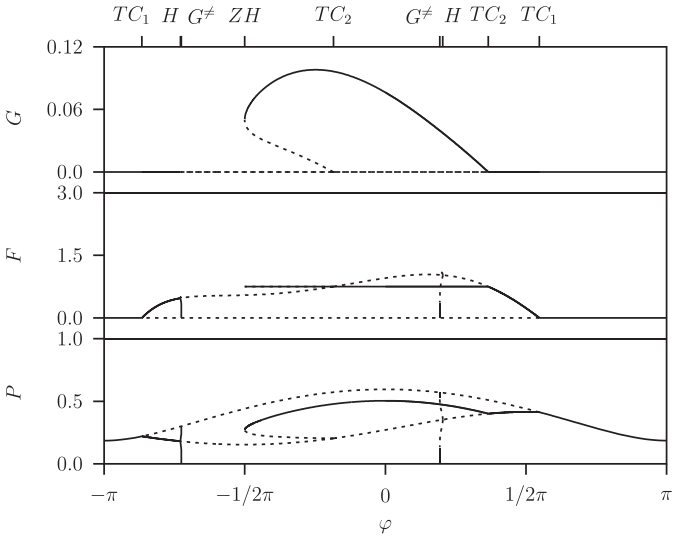

Fig. 8. One-parameter bifurcation diagram of endemic system (14), with the angle (φ) on the horizontal-axis, and the number of individuals in the populations *P*, *F*, *G* on the vertical-axis. The angle $\varphi \in [-\pi, \pi]$ is reckoned clockwise $(-\pi < \varphi < 0)$ and reckoned counter-clockwise $0 < \varphi < \pi)$ along an ellipse, given in (5), around the *TC-ZH-H* intersection point *M* at location ($K^* = 1.2147066$, $m^* = 0.13321752$).

6. Discussion

The demographic model (5) shows that the predators invade the system when the prey only equilibrium becomes unstable, i.e. for a small enough mortality rate $m < m^{\dagger}$, see (6) and (8) and the remark after these formulae.

The ecoepidemic model admits the origin, the prey-only and the coexistence equilibrium. We find in addition the predator–prey disease-free equilibrium corresponding to Q_2. The model with infected predators does not sustain an equilibrium with no healthy predators, but this is due to the assumptions of the model, namely the fact that infected predators are assumed to be too weak to perform any hunting activity.

The linear stability analysis of the origin shows it to be always unstable, a fact that would guarantee the survival of the ecosystem, but this would occur also for the disease-free model, thereby showing that this ecosystem behavior is due essentially to demographic reasons, due to the (possibly nondimensionalized) healthy prey reproduction rate that provides the positive eigenvalue responsible for the origin instability. However, the deeper nonlinear analysis of (Braza, 2012) and the findings of (Venturino and Petrovskii, 2013) of a stripe in the phase plane, for which trajectories are doomed to end up into the origin, see Fig. 7, indicate that the actual ecosystem behavior is prone to become extinct, in unfavorable circumstances, see region E_0 in Fig. 5. The prey in fact becomes extinct in finite time, followed by an exponential decay of the predators. This phenomenon is related to the presence of the square root terms in the HTII functional response.

The prey-only equilibrium through a transcritical bifurcation gives rise to the predator–prey disease-free equilibrium, whenever the predators' mortality rate falls below a certain threshold, $m_d^{\dagger}$. A close look at the shape of this threshold shows that the environment, through the prey carrying capacity, always influences the level of the threshold. The predators too contribute to this phenomenon, since their efficiency in hunting appears in the threshold expression, i.e. the parameter *a*. Note in fact that even in the purely demographic model, the constant t_h depends on the hunting rate, and in any case the converted prey parameter *c* appears explicitly in the definition of $m_d^{\dagger}$, (6).

The ecoepidemic case gives a slightly different form of the threshold. Through the parameter *e* the conversion process once again plays a role in $m^{\dagger}$ in the model (14) in which the disease affects the predators, see (15). This occurs together with the parameter *T* expressing the nondimensionalized prey capture time.

The bifurcation analyses revealed an organizing center point *M* in the two dimensional parameter space whereby *K* and *m* are the bifurcation parameters Figs. 4 and 5. Transcritical bifurcations *TC* show where by variation of a parameter the composition of the system changes because the predator invaded into a prey equilibrium or the predator population becomes infected, so from disease-free to endemic. At a Hopf bifurcation *H* the system changes the long-term dynamics qualitatively because it starts to oscillate instead of being in equilibrium. Also a zero-Hopf *ZH* bifurcation exists. Crossing this curve leads to a catastrophic phenomenon where all three populations go extinct (see Fig. 8). Furthermore, in a global bifurcation *G* a stable limit cycle disappears suddenly at a heteroclinic connection from a saddle

prey population equilibrium point E_1 to the zero-solution E_0 where the system collapses completely.

References

Ajraldi, V., Pittavino, M., Venturino, E., 2011. Modelling herd behavior in population systems. Nonlinear Anal. Real World Appl. 12, 2319–2338.

Bazykin, A.D., 1998. Nonlinear Dynamics of Interacting Populations. World Scientific, Singapore.

Beltrami, E., Carroll, T.O., 1994. Modelling the role of viral disease in recurrent phytoplankton blooms. J. Math. Biol. 32, 857–863.

Belvisi, S., Venturino, E., 2013. An ecoepidemic model with diseased predators and prey group defense. Simul. Model. Pract. Theory 34, 144–155.

Braza, P.A., 2012. Predator–prey dynamics with square root functional responses. Nonlinear Anal. Real World Appl. 13, 1837–1843.

Busenberg, S., Driessche van den, P., 1990. Analysis of a disease transmission model in a population with varying size. J. Math. Biol. 28, 257–270.

Chattopadhyay, J., Arino, O., 1999. A predator–prey model with disease in the prey. Nonlinear Anal. 36, 747–766.

Chattopadhyay, J., Chatterjee, S., Venturino, E., 2008. Patchy agglomeration as a transition from monospecies to recurrent plankton blooms. J. Theor. Biol. 253, 289–295.

Cosner, C., DeAngelis, D.L., Ault, J.S., Olson, D.B., 1999. Effects of spatial grouping on the functional response of predators. J. Theor. Biol. 56, 65–75.

Dhooge, A., Govaerts, W., Kuznetsov, Yu.A., 2003. Matcont: a MATLAB package for numerical bifurcation analysis of ODEs. ACM Trans. Math. Softw. 29, 141–164.

Doedel, E.J., Oldeman, B., 2009. Auto 07p: Continuation and Bifurcation Software For Ordinary Differential Equations, Technical Report. Concordia University, Montreal, Canada.

Freedman, H.I., Wolkowicz, G., 1986. Predator–prey systems with group defence: the paradox of enrichment revisited. Bull. Math. Biol. 48, 493–508.

Gimmelli, G., 2012. Modelli ecoepidemiologici con difesa di gruppo e saturazione (Ecoepidemiological models with group defense and saturation). University of Torino (Master thesis).

Guckenheimer, J., Holmes, P., 1985. Nonlinear Oscillations, Dynamical Systems and Bifurcations of Vector Fields, vol. 42 of Applied Mathematical Sciences, 2nd ed. Springer-Verlag, New York.

Hadeler, K.P., Freedman, H.I., 1989. Predator–prey populations with parasitic infection. J. Math. Biol. 27, 609–631.

Haque, M., Venturino, E., 2006. The role of transmissible diseases in Holling–Tanner predator–prey model. Theor. Popul. Biol. 70, 273–288.

Hethcote, H.W., 2000. The mathematics of infectious diseases. SIAM Rev. 42, 599–653.

Holling, C.S., 1965. The functional response of invertebrate predators to prey density. Mem. Entomol. Soc. Can. 45, 3–60.

Kooi, B.W., 2003. Numerical bifurcation analysis of ecosystems in a spatially homogeneous environment. Acta Biotheor. 51, 189–222.

Kuznetsov, Y.A., 2004. Elements of Applied Bifurcation Theory, vol. 112 of Applied Mathematical Sciences, 3rd ed. Springer-Verlag, New York.

Malchow, H., Petrovskii, S., Venturino, E., 2008. Spatiotemporal patterns in Ecology and Epidemiology. CRC, Boca Raton.

MATLAB Package, 2014. The MathWorks. Natick, Massachusetts, USA.

Mena-Lorca, J., Hethcote, H.W., 1992. Dynamic models of infectious diseases as regulator of population sizes. J. Math. Biol. 30, 693–716.

Romano, T., Banerjee, M., Venturino, E., 2014. A comparison of several plankton models for red tides. In: Kehayias, G. (Ed.), Zooplankton: Species Diversity, Distribution and Seasonal Dynamics. Nova Science Publishers, Hauppauge, New York, USA, pp. 1–47.

Saputra, K.V.I., van Veen, L., Quispel, G.R.W., 2010. The saddle-node-transcritical bifurcation in a population model with constant rate harvesting. Dyn. Continuous Discrete and Impulsive Syst. Ser. B: Math. Anal. 14, 233–250.

Tanner, J.T., 1976. The stability and intrinsic growth rates of prey and predator populations. Ecology 56, 855–867.

van Voorn, G.A.K., Hemerik, L., Boer, M.P., Kooi, B.W., 2007. Heteroclinic orbits indicate overexploitation in predator–prey systems with a strong Allee effect. Math. Biosci. 209, 451–469.

van Voorn, G.A.K., Kooi, B.W., Boer, M.P., 2010. Ecological consequences of global bifurcations in some food chain models. Math. Biosci. 226, 120–133.

van Voorn, G.A.K., Kooi, B.W., 2013. Smoking epidemic eradication in a eco-epidemiological dynamical model. Ecol. Complex. 14, 180–189.

Venturino, E., 1994. The influence of diseases on Lotka–Volterra systems. Rocky Mountain J. Math. 24, 381–402.

Venturino, E., 1995. Epidemics in predator–prey models: disease among the prey. In: Arino, O., Axelrod, D., Kimmel, M., Langlais, M. (Eds.), Mathematical Population Dynamics: Analysis of Heterogeneity, vol. 1: Theory of Epidemics. Wuertz Publishing Ltd, Winnipeg, Canada, pp. 381–393.

Venturino, E., 2011. A minimal model for ecoepidemics with group defense. J. Biol. Syst. 19, 763–785.

Venturino, E., Petrovskii, S., 2013. Spatiotemporal behavior of a prey-predator system with a group defense for prey. Ecol. Complex. 14, 37–47.

Wiggins, S., 1988. Global Bifurcations and Chaos: Analytical Methods. Springer-Verlag, New York.

Wiggins, S., 1990. Introduction to Applied Nonlinear Dynamical Systems and Chaos, vol. 2 of Texts in Applied Mathematics Springer-Verlag, New York.